Received 1 August 2018; revised 16 September 2018 and 21 September 2018; accepted 22 September 2018. Date of publication 1 October 2018; date of current version 8 March 2019. The review of this paper was arranged by Editor M. Chan.

*Digital Object Identifier 10.1109/JEDS.2018.2872714*

# Rapidly Measuring Charge Carrier Mobility of Organic Semiconductor Films Upon a Point-Contact Four-Probes Method

**DONGFAN LI, SHENGTAO LI (Senior Member, IEEE), WANLONG LU, SHI FENG, PENG WEI, YUPENG HU, XUDONG WANG, AND GUANGHAO LU**

Frontier Institute of Science and Technology, State Key Laboratory of Electrical Insulation and Power Equipment, Xi'an Jiaotong University, Xi'an 710054, China

CORRESPONDING AUTHOR: D. LI (e-mail: dongfan.li@foxmail.com), S. LI (e-mail: sli@mail.xjtu.edu.cn), and G. Lu (e-mail: guanghao.lu@mail.xjtu.edu.cn)

This work was supported in part by the Natural Science Foundation of China under Grant 51473132, and in part by the Youth 1000 Plan Program of China. The work of G. Lu was supported in part by the Fundamental Research Funds for the Central Universities and in part by Cyrus Tang Foundation.

**ABSTRACT** Field-effect mobility ($\mu_{FET}$) of organic semiconductor films plays a key role in the performance of field-effect transistors (FETs). Numerical extraction of $\mu_{FET}$ from organic FET characteristics is not only time-consuming due to patterning of source/drain electrodes, but also frequently unreliable because of the contact resistances ($R_C$) between source/drain electrodes and semiconductors. Here, we propose an approach to rapidly evaluate $\mu$ by a point-contact four-probes method ($\mu_{PFP}$) for organic semiconductor films. Four tip-like probes quickly contact the semiconductor film surface directly, without deposition of the conventional source/drain electrodes, to simultaneously inject current and measure the electric potential. The charge density and thus conductance of the film is manipulated upon scanning gate voltage, from which the extraction of $\mu_{PFP}$, in good agreement with $\mu_{FET}$, could be realized in a few seconds. This method, with easily accessible setup and numerical model, substantially accelerates the evaluation of $\mu_{PFP}$, and thus could help screen materials and optimize film morphology for organic FETs applications.

**INDEX TERMS** Organic semiconductor films, charge carrier mobility, point-contact four-probes method.

## I. INTRODUCTION

The field-effect mobility plays a key role in the performance of field-effect transistors (FETs) [1]–[6], which is usually numerically extracted from FETs characteristics [7]–[9]. However, $R_C$ between source/drain electrodes and semiconductor layers, which may depend on gate voltage ($V_G$) [10], greatly has influenced the performance of FETs, and frequently leads to either underestimation or overestimation of $\mu_{FET}$ [11]–[17]. The influences of $R_C$ on mobility extraction can be largely eliminated by using four-probes method, which allows to gain a more comprehensive understanding about the intrinsic charge transport behavior.

In a typical four-probes architecture for FETs, two individual electrodes are deposited in the semiconductor channel area between source and drain electrodes [15], [18]–[20] to measure the electric potential drop across the channel area. This method, which requires patterning of four electrodes, is rather time-consuming and not environmental friendly. Alternatively, other creative methods for measuring the charge carrier mobility of some organic films, by means of scanning tunneling microscope [21], [22] or scanning Kelvin-probe force microscopy [23], is even more inaccessible for conventionally-equipped labs. Thus, the rapid evaluation of mobility using easily-accessible setup and appropriate charge transport model, without necessarily deposition of conventional electrodes, is highly attractive.

Actually, an existing point-contact four-probes method upon directly mounting four conducting tips on material surface is being widely used for measuring electrical conductivity for materials with relatively low resistance [22], [23]. Moreover, a four probes contact technique, which was directly modified from this method, was utilized to evaluate

the field-effect behavior for silicon on insulator [24], [25]. This is an inorganic material. However, due to the typically low mobility for organic semiconductor thin-films and tiny film thickness (usually a few tens of nanometers), it was usually believed that the electrical resistance of such thin-films is usually too high to apply such a point-contact four-probes method, even under a moderate gate voltage. In fact, the probes usually damage the underneath soft organic materials, and even though the contacts between probes and organic materials could be too loose to warrant enough charge injection and reliable potential measurements. Fortunately, in the past decades the mobility of organic semiconductor films has been greatly improved to be $> 10\ \mathrm{cm^2V^{-1}s^{-1}}$ [3], [26]–[28]. The sheet resistance of the film, which depends on charge density and mobility, could be reduced to a reasonably low value under a certain range of gate voltage. In principle, this could potentially allow us to use conventional lab electric instruments and four point-contacts to inject sufficient current into the film and directly measure the potential distribution along the film, without fabrication of entire FETs via deposition of conventional source/drain electrodes. Taking this consideration into account, here, we propose a rapid approach to directly measure the mobility of semiconductor films using a point-contact four-probes method in ambient.

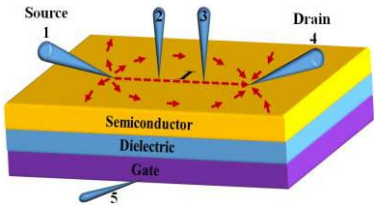


**FIGURE 1. The scheme of the point-contact four-probes method. The number 1, 2, 3 and 4 show the four point-contact probes, and 5 represents gate electrode. Current is injected from 1 towards 4, and we use 2 and 3 to measure the potential. The red arrows schematically denote the current directions.**

In this work, four flexible Be-Cu tips coated with graphite powder are used as probes. As shown in Fig. 1, probe 1 and 4 are used to supply constant channel voltage (the current is $I_{14}$) by Agilent B2902A, which replaces the source and drain electrodes, respectively. Note that probe 1 is grounded, $V_1 = V_S = 0$ V, $V_4 = V_D$. Probe 2 and 3 are used to measure the electrical point potential ($V_{12}$ and $V_{13}$) in the conductive channel by two independent KEITHLEY 2000, respectively. Note that $V_{23} = V_{12}$- $V_{13}$. We use doping to reduce the contact resistance. In fact, the Eq. (13) would avoid the potential drop induced by contact resistance. In view of the equipment condition, four flexible Be-Cu tips coated with graphite powder are used as probes, which provides a possibility to be non-invasive contact. This drastically reduces the unnecessary cost and saves much time, simultaneously. Probe 5 is connected to the gate to provide $V_G$ by KEITHLEY 6517B. For the p-type FETs, $|V_G - V_T| > |V_{DS}|$ is used to make the device works well in linear region and the electrical conductance of the film is sufficient for the measurement.

## II. EXPERIMENTAL

The Organic semiconductor 2,7-didodecyl [1] benzothieno [3,2-b] [1] benzothiophene ($C_{12}$-BTBT) and the dopant hexacyano-trimethylene-cyclopropane were synthesized in our laboratory. Polystyrene (PS) (Sigma Aldrich, Inc.) was dissolved in o-dichlorobenzene with a concentration of 5 mg/ml, and the solution was spin-coated at 2000 rpm for 120 s onto the clean substrate wafers with 300 nm-thick thermal oxide layer, of which the thickness of PS measured by us is about 20nm, which is much more thinner compared to the 300 nm-thick $SiO_2$ layer.

$$C = \frac{\varepsilon_0 \varepsilon_r}{d} \tag{1}$$

where $C$ is the capacitance per unit area of dielectric layer, $\varepsilon_0$ is relative dielectric constant, $\varepsilon$ is the dielectric constant and $d$ is the thickness. Based on the capacitance formula presented above, it's easy to know that the $C_{PS}$ is much larger than $C_{SiO2}$. In the architecture of OFET, the total capacitance can be approximately regarded as the $C_{SiO2}$. Subsequently, $C_{12}$-BTBT was then thermally evaporated at a speed of 0.1 Å/s to obtain 30 nm-thick semiconductor films (under $\sim 6\times10^{-4}$ Pa) on the PS layer. Then the dopant was thermally evaporated at a speed of 0.1 Å/s to obtain 1 nm-thick films on the semiconductor layer (under $\sim 6\times10^{-4}$ Pa). The film could be used directly for mobility measurement upon point-contact four-probes method. As for control experiments, for conventional FETs, the source and drain electrodes were thermally deposited onto the doped semiconductor film in vacuum through a shadow mask, with a channel width ($W$) of 3000 μm and channel length ($L$) ranging from 50 μm to 300 μm, respectively.

## III. RESULTS AND DISCUSSIONS

The transfer and output characteristics of the conventional FETs are shown in Fig. 2(a) - (b). The threshold voltage of the device is $\sim$ 0 V, which indicates the powerful p type dopant. Considering the measurement limitation of our instruments, we choose -20 V of $V_D$. Smaller drain bias would lead to smaller current and smaller potential drop, which would yield more errors. On the other hand, we can think that the device is operating in linear regime according to the relationship of $|V_G - V_T| > V_{SD}$. Here, $V_T$ is $\sim$ 0 V, as mentioned above. Though the linear regime not critical when $V_D$ = -20 V, but reliable enough. Fig. 3(b) shows the dependence of $\mu_{FET}$ on the $V_G$, which is obtained from the differential form of conventional $I$-$V$ equation in linear regime

$$\mu = \frac{L}{WCV_{SD}} \frac{\partial I_{SD}}{\partial V_G} \tag{2}$$

$\mu_{FET}$ increases monotonously with the increase of $|V_G|$(from 40 V to 70 V). Abrupt drop occurs when $|V_G|$ increases further to 80 V, which is attributed to the $R_C$ [11], [28], [29].

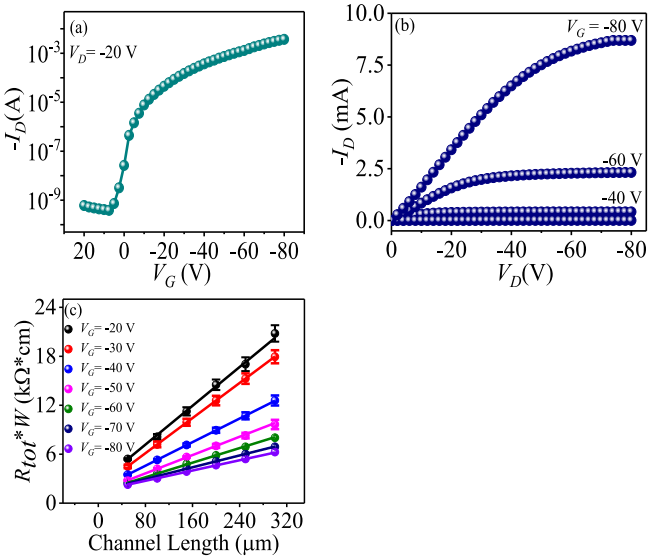


**FIGURE 2.** **The OFETs' performance of $C_{12}$-BTBT thin film with doping. The channel length and width are 50 $\mu$m and 3000 $\mu$m, respectively. (a) The transfer characteristics. (b) The output characteristics. (c) Dependence of width-normalized total resistance $R_{TOT}$*$W$ on channel length.**

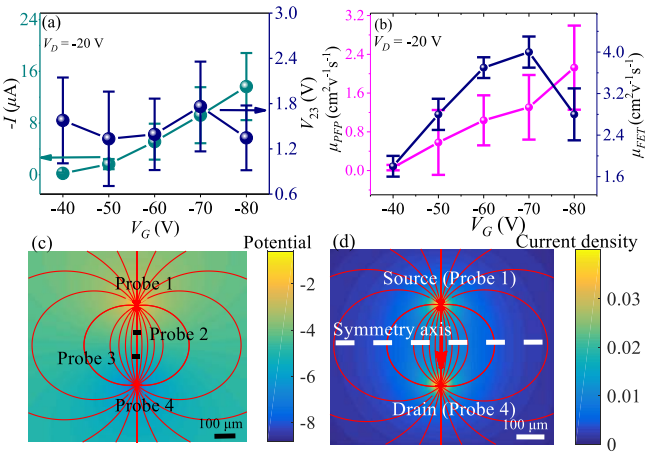


**FIGURE 3.** **Measuring the mobility upon point-contact four-probes method. (a) Dependence of $I$ and $V_{23}$ on $V_G$. (b) Dependence of $\mu_{FET}$ on $V_G$ extracted directly from transfer curves in linear regime as shown in Fig. 2(a) and the relationship of $\mu_{PFP}$ vs. $V_G$, respectively. (c, d) Simulated in-plane potential (c, unit is V) and current density distribution (d, unit is $\mu$A/$\mu$m) contours when the film is measured upon point-contact four-probes method ($V_{12}$ = 3 V, $V_G$= -80 V). The solid lines in (c) and (d) represent current density streamlines. The arrow in (d) shows the current direction.**

Moreover, $R_C$ was measured by transfer line method [30]. Fig. 2(c) shows channel width-normalized total resistances ($R_{TOT}$*$W$) versus channel length for various $V_G$, where $R_{TOT}$ is the total resistance including $R_C$ and channel resistance. The device total resistance scales linearly with channel length. The linear dependence of the $R_{TOT}$*$W$ can be extrapolated to the y-axis intercept, which is below 1 KΩ cm.

Subsequently, based on the conventional $I$-$V$ equation in linear regime, we propose a simple model to calculate the field-effect mobility according to the point-contact four-probes architecture. Here, probe 1 and probe 4 can be seen as the source and drain electrodes, respectively, which means that the current flows in the conductive channel from probe 1 towards probe 4. Note that probe 1 is grounded, that is, $V_1 = V_S = 0$ V, $V_4 = V_D$, where $V_S$ and $V_D$ denotes the source and drain potential, respectively. The differential form of linear zone channel current-voltage equation can be expressed:

$$I = \frac{2\pi r}{dr}\mu C(V_G - V - \frac{dV}{2})dV \tag{3}$$

Neglect the second order infinitesimal:

$$I = \frac{2\pi r}{dr}\mu C(V_G - V)dV \tag{4}$$

Transform, and then:

$$\frac{1}{r}dr = \frac{2\pi\mu}{I}C(V_G - V)dV \tag{5}$$

Then, the effect of probe 1 on the two dimensional plane at any point $x$:

$$\frac{dr_1}{r_1} = \frac{2\pi C\mu}{I}[V_G - V_{Sx} - V_{Dx})]dV_{Sx} \tag{6}$$

where $r_1$ denotes the distance between probe 1 and point $x$, $I$ is the channel current. $V_{Sx}$ and $V_{Dx}$ denote the potential difference between source (probe 1)/ drain (probe 4) and planar arbitrary point $x$, respectively. These electrical parameter, such as point potential and current in conductive channel under different $V_G$ can be read out through the electricity meter. The effect of probe 4 on the plane at any point $x$ is similar to Eq. (6), taking the current direction into consideration:

$$\frac{dr_4}{r_4} = \frac{2\pi C\mu}{-I}[V_G - V_{Sx} - V_{Dx})]dV_{Dx} \tag{7}$$

From Eq. (6) and Eq. (7), the synergistic effect of probe 1 (source) and probe 4 (drain) on point $x$ can be obtained:

$$\frac{dr_1}{r_1} - \frac{dr_4}{r_4} = \frac{2\pi C\mu}{I}(V_G - V)dV \tag{8}$$

Here, $V = V_S + V_D$. Take infinity as potential energy zero, Eq. (8) can be then integrated to be:

$$\int_0^V \frac{2\pi C\mu}{I}(V_G - V)dV = \int_{r_1\to\infty}^{r_{1x}} \frac{dr_1}{r_1} - \int_{r_4\to\infty}^{r_{4x}} \frac{dr_4}{r_4} = \ln\frac{r_{1x}}{r_{4x}} \tag{9}$$

Based on Eq. (9), the synergistic effect of probe 1 (source) and probe 4 (drain) on probe 2 and probe 3 can be written as:

$$\ln\frac{r_{42}}{r_{12}} = \frac{2\pi C\mu}{I}\left(V_G V_{12} - \frac{V_{12}^2}{2}\right) \tag{10}$$

and

$$\ln\frac{r_{43}}{r_{13}} = \frac{2\pi C\mu}{I}\left(V_G V_{13} - \frac{V_{13}^2}{2}\right), \tag{11}$$

respectively. Combined with the Eq. (10) and Eq. (11):

$$\ln\frac{r_{42}r_{13}}{r_{12}r_{43}}=\frac{2\pi C\mu}{I}\left[V_{\mathrm{G}}V_{23}-\frac{V_{23}(V_{12}+V_{13})}{2}\right] \quad (12)$$

From Eq. (12), the channel field-effect mobility (denoted as $\mu_{\mathrm{PFP}}$) in the region between the point 2 and 3 can be obtained:

$$\mu_{\mathrm{PFP}}=\frac{I}{V_{23}}\frac{1}{2\pi C}\frac{\ln\frac{r_{24}r_{13}}{r_{12}r_{34}}}{V_{\mathrm{G}}-\frac{V_{12}+V_{13}}{2}} \quad (13)$$

The point-contact four-probes method experiment data is shown in Fig. 3(a). The channel current increases with the increase of -$V_{\mathrm{G}}$, whereas no obvious changes of $V_{23}$ are observed. The voltage drop in $V_{23}$ is around 10% for $V_{\mathrm{D}}$, which is a reasonable value because at high gate-voltage and low drain-voltage, most of the potential drop is around probe 1 and probe 4, as simulated in Fig. 3(c). These potential drops are not due to the contact resistances, because the contact area of the tip is small and thus the resistance of the film around the tips are high.

$C_{12}$-BTBT is chosen as our semiconducting material for its high mobility performance with excellent air stability. However, the film prepared by us is polycrystalline [7], which leads to a dispersive voltage drop of $V_{23}$ for different numbers of grain boundaries between probe 1 and probe 4 in every measurement. Therefore, the result seems noisy, but it is indeed due to the morphological dispersity. Actually, the contact resistance is lowered by doping. In addition, the $\mu_{\mathrm{PFP}}$ is approaching to $\mu_{\mathrm{FET}}$ as they are at least in the same order of magnitude, which is indirectly proves the certain reliability of $V_{23}$.

The conductivity of the materials is proportional to mobility and charge density. In our manuscript, we use high-mobility organic semiconductor $C_{12}$-BTBT in combination with strong dopant hexacyano-trimethylene-cyclopropane, the latter of which is known to be among the most efficient organic dopants for organic semiconductors. The LUMO level of hexacyano-trimethylene-cyclopropane is much lower than that of the well-known dopant $F_4$TCNQ [31]. Therefore, the doping could induce sufficient charge density to guarantee low resistance for the measurement, especially at high -$V_{\mathrm{G}}$. In our measurements, due to the size of the contact area of tips is about 0.3mm, the resistance between tips could easily reach less than MΩ once the gate voltage is high enough.

While we do not claim that our method could be used for every organic semiconductor, what we believe is that our method is available for high-mobility materials especially at high gate-voltage because in such cases the resistances of films are low enough. Fortunately, in the community of organic electronics, currently more and more high-mobility materials have been developed, which are attracting more attention than low-mobility materials. Consequently, we are very confident that our method could warrant its application in near future.

The dependence of mobility $\mu_{\mathrm{PFP}}$ on gate-voltage is obtained [see Fig. 3(b)], which shows that the $\mu_{\mathrm{TFT}}$ and the $\mu_{\mathrm{PFP}}$ don't match well. Possible reasons are as follows. First, the two charge carrier mobilities are obtained from two different models, of which are based on different assumptions. That is, $\mu_{\mathrm{TFT}}$ is derived from parallel plate capacitor model, whereas, $\mu_{\mathrm{PFP}}$ is based on point charge model. Due to tail states, the increase of $\mu_{\mathrm{PFP}}$ with $V_{\mathrm{G}}$ is found. To simplify the equation, location independent $\mu_{\mathrm{PFP}}$ is assumed. In addition, the golden electrodes and Be-Cu coated with graphite powder is different, which may result in different mobilities. However, we can see that the $\mu_{\mathrm{PFP}}$ is at least in the same order of magnitude with $\mu_{\mathrm{FET}}$. Note that the $\mu_{\mathrm{PFP}}$ is obtained from Eq. (13). Besides, the sudden decrease of field-effect mobility with a further increase of -$V_{\mathrm{G}}$ (approximately from -70 V to -80 V) is not present, which may indirectly prove that the negative impact caused by contact resistance can be effectively eliminated by using point-contact four-probes method. Moreover, suppose the equal distance between the four probes, that is, $r_{12}=r_{43}$, $r_{42}=r_{13}$, $r_{42}=2r_{12}$. Meanwhile, $V_{12}$ ($V_{13}$) is much smaller than -$V_{\mathrm{G}}$ under a high gate bias (> -40 V), the Eq. (13) can be simplified as:

$$\mu_{\mathrm{PFP}}\approx\frac{I}{V_{23}}\frac{\ln 2}{\pi CV_{\mathrm{G}}} \quad (14)$$

We can evaluate the field-effect mobility roughly from Eq. (14), which shows a rapid and reliable evaluation. The simple experimental setup and Eq. (14) is practically applicable for rapid evaluation of mobility of organic semiconductor thin films.

From Eq. (9), the equation for contour on the two-dimensional plane:

$$\ln\frac{\sqrt{(x-x_1)^2+(y-y_1)^2}}{\sqrt{(x-x_4)^2+(y-y_4)^2}}=\frac{2\pi C\mu}{I}\left(V_{\mathrm{G}}V_{\mathrm{SX}}-\frac{V_{\mathrm{SX}}^2}{2}\right) \quad (15)$$

where ($x$, $y$) denotes the coordinate of arbitrary point in this plane, ($x_1$, $y_1$) and ($x_4$, $y_4$) represents the coordinate of point 1 and 4, respectively. The potential distribution and current density streamlines in OFETs are obtained from a two-dimensional finite element analysis by solving Eq. (15) according to the experiment data [see Fig. 3(c)]. The current density is the highest near the region of point 1 and 4, and decreases as the current path lengthens, as is shown in Fig. 3(d). As can be seen from this image, the current passes perpendicularly through the symmetry axis of the two current probes (probe 1 and probe 4) in this geometry. In this case, as represented in the simulation of Fig. 3(c) and Fig. 3(d), the potential linearly drops when current flows from probe 1 to 4. The scale bar is 100 $\mu$m long.

Although four-probe method, which was directly modified from the method widely used for four-probes electrical conductivity measurement, has been used to evaluate the field-effect behavior in inorganic material [24], [25]. Our numerical derivation, as shown in detail in Eq. (3)-(13), represents a more universal treatment. Upon simulating the electrical potential and current distribution contours

(Fig. 3(c)-(d)), we show that various of measurement architectures could be available for different cases, that is, the four-probes are not necessarily aligned within a line but could be mounted in other places on the film plane to measure the potential evolution.

Our method, for the first time, proves that rapid evaluation of field-effect mobility of organic semiconductors is possible by four-probes method. From the material point of view, organic semiconductors are featured with noncovalent interactions between molecules, leading to a different charge transport scenario from that in inorganic materials. As the mobility of increasing organic semiconductor films has been greatly improved over 10 $cm^2V^{-1}s^{-1}$, our method could be widely used in this community.

In fact, the field-effect mobility of organic semiconductors is frequently gate-voltage-dependent, and usually shows a bislope feature [3], [12], [13], [19], which is different from the charge transport in inorganic materials. As shown in the experimental results [Fig. 3(b)], the field-effect mobility of BTBT measured by our method monotonically increases with gate-voltage, and does not demonstrate bislope behavior. This implies that the bislope behavior of field-effect mobility commonly observed in real transistors is due to the gate-voltage-dependent contact resistance.

## IV. CONCLUSION

In this work, a fast and easily-accessible method is proposed to directly measure the charge carrier mobility of organic semiconductor thin film. The four tip-like probes are simply mounted onto the semiconductor film surface directly to form four point-contacts, without deposition of extra source/drain electrodes. Unlike the conventionally patterned source/drain electrodes, the tip-like probes are not disposable materials and thus could be repeatedly used for many other measurements. We focus on estimating mobility organic semiconducting films that is at least in the same order of magnitude with $\mu_{FET}$ by using a faster and affordable alternative to methods like STM and kelvin-probe microscopy. This method, with easily-accessible setup and convincing numerical model, substantially accelerates the evaluation of $\mu_{PFP}$, and thus could be widely used to screen materials and optimize film morphology for organic FETs applications.

## ACKNOWLEDGMENT

The authors are grateful to Dr. Prof. Martin Heeney, Dr. Prof. Norbert Koch, Dr. Prof. Osuji, Dr. Prof. Hayward, Dr. Ben Bin Xu, Dr. Prof. Xiaojie Lou, Dr. Prof. Yanhou Geng, Han Yu, Botao Liu, and Chongjian Tang for experimental assistance and fruitful discussion.

## REFERENCES

[1] G. Lu *et al.*, "Dual-characteristic transistors based on semiconducting polymer blends," *Adv. Electron. Mater.*, vol. 2, no. 10, pp. 1–7, Aug. 2016, doi: 10.1002/aelm.201600267.

[2] C. Qian *et al.*, "High-performance organic heterojunction phototransistors based on highly ordered copper phthalocyanine/para-sexiphenyl thin films," *Adv. Funct. Mater.*, vol. 27, no. 6, pp. 1–8, Dec. 2017, doi: 10.1002/adfm.201604933.

[3] Y. Yuan *et al.*, "Ultra-high mobility transparent organic thin film transistors grown by an off-centre spin-coating method," *Nat. Commun.*, vol. 5, pp. 1–9, Jan. 2014, doi: 10.1038/ncomms4005.

[4] L. Bu, M. Hu, W. Lu, Z. Wang, and G. Lu, "Printing semiconductor-insulator polymer bilayers for high-performance coplanar field-effect transistors," *Adv. Mater.*, vol. 30, no. 2, pp. 1–9, Nov. 2018, doi: 10.1002/adma.201704695.

[5] H. Qiu *et al.*, "Electrical characterization of back-gated bi-layer $MoS_2$ field-effect transistors and the effect of ambient on their performances," *Appl. Phys. Lett.*, vol. 100, no. 12, pp. 1–3, Mar. 2012, doi: 10.1063/1.4801861.

[6] J. C. Bijleveld *et al.*, "Poly (diketopyrrolopyrrole-terthiophene) for ambipolar logic and photovoltaics," *J. Amer. Chem. Soc.*, vol. 131, no. 46, pp. 16616–16617, Nov. 2009, doi: 10.1021/ja907506r.

[7] P. Wei *et al.*, "Organic-semiconductor: Polymer-electret blends for high-performance transistors," *Nano Res.*, pp. 1–14, May 2018, doi: 10.1007/s12274-018-2088-7.

[8] C.-I. Yang *et al.*, "Drain-induced-barrier-lowing-like effect induced by oxygen-vacancy in scaling-down via-contact type amorphous InGaZnO thin-film transistors," *IEEE J. Electron Devices Soc.*, vol. 6, pp. 685–690, May 2018, doi: 10.1109/JEDS.2018.2837682.

[9] M. Mativenga, H. Jun, Y. Choe, J. G. Um, and J. Jang, "Circular structure for high mechanical bending stability of a-IGZO TFTs," *IEEE J. Electron Devices Soc.*, vol. 5, no. 6, pp. 453–457, Nov. 2017, doi: 10.1109/JEDS.2017.2751651.

[10] L. Zhou, L. Bu, D. Li, and G. Lu, "Gate-voltage-dependent charge transport in multi-dispersed polymer thin films," *Appl. Phys. Lett.*, vol. 110, no. 9, pp. 1–5, Feb. 2017, doi: 10.1063/1.4977436.

[11] I. McCulloch, A. Salleo, and M. Chabinyc, "Avoid the kinks when measuring mobility," *Science*, vol. 352, no. 6293, pp. 1521–1522, Jun. 2016, doi: 10.1126/science.aaf9062.

[12] C. Liu *et al.*, "Device physics of contact issues for the overestimation and underestimation of carrier mobility in field-effect transistors," *Phys. Rev. Appl.*, vol. 8, no. 3, pp. 1–10, Sep. 2017, doi: 10.1103/PhysRevApplied.8.034020.

[13] R. D. Pietro *et al.*, "Simultaneous extraction of charge density dependent mobility and variable contact resistance from thin film transistors," *Appl. Phys. Lett.*, vol. 104, no. 19, pp. 1–5, May 2014, doi: 10.1063/1.4876057.

[14] D. Venkateshvaran *et al.*, "Approaching disorder-free transport in high-mobility conjugated polymers," *Nature*, vol. 515, no. 7527, pp. 384–388, Nov. 2014, doi: 10.1038/nature13854.

[15] H. H. Choi *et al.*, "Accurate extraction of charge carrier mobility in 4-probe field-effect transistors," *Adv. Funct. Mater.*, vol. 28, no. 26, pp. 1–11, Apr. 2018, doi: 10.1002/adfm.201707105.

[16] H. H. Choi, K. Cho, C. D. Frisbie, H. Sirringhaus, and V. Podzorov, "Critical assessment of charge mobility extraction in FETs," *Nat. Mater.*, vol. 17, no. 1, pp. 2–7, Dec. 2017, doi: 10.1038/nmat5035.

[17] Y. Hu, G. Li, W. Peng, and Z. Chen, "Comparing the gate dependence of contact resistance and channel resistance in organic field-effect transistors for understanding the mobility overestimation issue," *IEEE Electron Device Lett.*, vol. 39, no. 3, pp. 421–423, Jan. 2018, doi: 10.1109/LED.2018.2798288.

[18] V. C. Sundar *et al.*, "Elastomeric transistor stamps: Reversible probing of charge transport in organic crystals," *Science*, vol. 303, no. 5664, pp. 1644–1646, Mar. 2004, doi: 10.1126/science.1094196.

[19] C. Rolin *et al.*, "Charge carrier mobility in thin films of organic semiconductors by the gated van der Pauw method," *Nat. Commun.*, vol. 8, pp. 1–9, Apr. 2017, doi: 10.1038/ncomms14975.

[20] T. Minari, T. Miyadera, K. Tsukagoshi, Y. Aoyagi, and H. Ito, "Charge injection process in organic field-effect transistors," *Appl. Phys. Lett.*, vol. 91, no. 5, Aug. 2007, Art. no. 053508, doi: 10.1063/1.2759987.

[21] R. Ma *et al.*, "Direct four-probe measurement of grain-boundary resistivity and mobility in millimeter-sized graphene," *Nano Lett.*, vol. 17, no. 9, pp. 5291–5296, Aug. 2017, doi: 10.1021/acs.nanolett.7b01624.

[22] S. Yoshimoto *et al.*, "Highly anisotropic mobility in solution processed TIPS-pentacene film studied by independently driven four GaIn probes," *Appl. Phys. Lett.*, vol. 111, no. 7, Aug. 2017, Art. no. 073301, doi: 10.1063/1.4998949.

[23] V. Milotti, M. Pietsch, K. P. Strunk, and C. Melzer, "Measuring the lateral charge-carrier mobility in metal-insulator-semiconductor capacitors via Kelvin-probe," *Rev. Sci. Instrum.*, vol. 89, no. 1, pp. 1–6, Jan. 2018, doi: 10.1063/1.5002629.
[24] S. Cristoloveanu and S. Williams, "Point-contact pseudo-MOSFET for in-situ characterization of as-grown silicon-on-insulator wafers," *IEEE Electron Device Lett.*, vol. 13, no. 2, pp. 102–104, Feb. 1992, doi: 10.1109/55.144972.
[25] A. M. Ionescu and D. Munteanu, "A novel in-situ SOI characterization technique: The intrinsic point-probe MOSFET," *IEEE Electron Device Lett.*, vol. 22, no. 4, pp. 166–169, Apr. 2001, doi: 10.1109/55.915601.
[26] H. Minemawari *et al.*, "Inkjet printing of single-crystal films," *Nature*, vol. 475, no. 7356, pp. 364–367, Jul. 2011, doi: 10.1038/nature10313.
[27] C. Luo *et al.*, "General strategy for self-assembly of highly oriented nanocrystalline semiconducting polymers with high mobility," *Nano Lett.*, vol. 14, no. 5, pp. 2764–2771, Apr. 2014, doi: 10.1021/nl500758w.
[28] E. G. Bittle, J. I. Basham, T. N. Jackson, O. D. Jurchescu, and D. J. Gundlach, "Mobility overestimation due to gated contacts in organic field-effect transistors," *Nat. Commun.*, vol. 7, pp. 1–7, Mar. 2016, doi: 10.1038/ncomms10908.
[29] T. Uemura *et al.*, "On the extraction of charge carrier mobility in high-mobility organic transistors," *Adv. Mater.*, vol. 28, no. 1, pp. 151–155, Nov. 2016, doi: 10.1002/adma.201503133.
[30] C. H. Kim, Y. Bonnassieux, and G. Horowitz, "Charge distribution and contact resistance model for coplanar organic field-effect transistors," *IEEE Trans. Electron Devices*, vol. 60, no. 1, pp. 280–287, Nov. 2013, doi: 10.1109/TED.2012.2226887.
[31] Y. Karpov *et al.*, "High conductivity in molecularly p-doped diketopyrrolopyrrole-based polymer: The impact of a high dopant strength and good structural order," *Adv. Mater.*, vol. 28, no. 28, pp. 6003–6010, May 2016, doi: 10.1002/adma.201506295.

**DONGFAN LI** received the B.S. and M.S. degrees from Northwestern Polytechnical University, China. He is currently pursuing the Ph.D. degree with the Frontier Institute of Science and Technology and State Key Laboratory of Electrical Insulation and Power Equipment, Xi'an Jiaotong University, China.

**SHENGTAO LI** (M'96–SM'11) received the Ph.D. degree in electrical engineering from Xi'an Jiaotong University (XJTU) in 1990, where he was a Lecturer, an Associate Professor, and a Professor in 1990, 1993, and 1998, respectively. From 1993 to 2003, he was the Deputy Director of the State Key Laboratory of Electrical Insulating and Power Equipment (SKLEIPE), XJTU, where he has been the Executive Deputy Director of SKLEIPE since 2003. Since 2013, he has been the Deputy Dean of the Department of Electrical Engineering, XJTU. He received financial support from the National Science Foundation for Distinguished Young Scholars of China in 2006. His research interests include dielectrics and their application, insulating materials, and electrical insulation. He is an Associate Editor of the IEEE TRANSACTIONS ON DIELECTRICS AND ELECTRICAL INSULATING.

**WANLONG LU** received the B.S. degree from Lanzhou University, Lanzhou, China, in 2015. He is currently pursuing the Ph.D. degree with the Frontier Institute of Science and Technology, Xi'an Jiaotong University.

**SHI FENG** received the B.S. degree in physics from Xi'an Jiaotong University, Xi'an, China, in 2018. He is currently pursuing the Ph.D degree in physics with Ohio State University, Columbus, USA. His current research interests include quantum hall effect, quantum gas, and Bose–Einstein condensation in ultracold atoms.

**PENG WEI** received the B.S. degree from the School of Materials Science and Engineering, Xi'an Jiaotong University, Xi'an, China, in 2016, where he is currently pursuing the Ph.D. degree with the Frontier Institute of Science and Technology.

**YUPENG HU** received the B.S. degree in applied physics from Xian Jiaotong University in 2016, where he is currently pursuing the M.S. degree in condense matter physics. His research interests are the simulation for flexible electronics devices, such as OFET and Solar Cell.

**XUDONG WANG** received the B.S. and M.S. degrees from Tsinghua University, China, in 2012 and 2015, respectively. He is currently a Research Assistant with the Frontier Institute of Science and Technology, Xi'an Jiaotong University, China. His research interests include density functional theory for electronic materials and applications, such as phase change materials for memories and topological insulators.

**GUANGHAO LU** received the bachelor's degree from Nanjing University in 2004 and the Ph.D. degree from the Changchun Institute of Applied Chemistry, Chinese Academy of Sciences in 2010. He was a Post-Doctoral Researcher in Germany and USA from 2010 to 2014. He joined the Frontier Institute of Science and Technology, Xi'an Jiaotong University in 2014. His research interest focuses on charge transport in semiconductors and insulators for organic electronics.